Transport of Vesicular Stomatitis Virus G Protein to the Cell Surface Is Signal Mediated in Polarized and Nonpolarized Cells

Anne Müsch,* Huaxi Xu,‡ Dennis Shields,‡ and Enrique Rodriguez-Boulan*

*Department of Cell Biology, Cornell University Medical School, 1300 York Avenue, New York, New York 10021; and ‡Department of Developmental and Molecular Biology, Anatomy and Structural Biology, Albert Einstein College of Medicine, 1300 Morris Park Avenue, Bronx, New York 10461

Abstract. Current models propose that in nonpolarized cells, transport of plasma membrane proteins to the surface occurs by default. In contrast, compelling evidence indicates that in polarized epithelial cells, plasma membrane proteins are sorted in the TGN into at least two vectorial routes to apical and basolateral surface domains. Since both apical and basolateral proteins are also normally expressed by both polarized and nonpolarized cells, we explored here whether recently described basolateral sorting signals in the cytoplasmic domain of basolateral proteins are recognized and used for post-TGN transport by nonpolarized cells. To this end, we compared the inhibitory effect of basolateral signal peptides on the cytosol-stimulated release of two basolateral and one apical marker in semi-intact fibroblasts (3T3), pituitary (GH3), and epithelial (MDCK) cells. A basolateral signal peptide (VSVGp) corresponding to the 29–amino acid cytoplasmic tail of vesicular stomatitis virus G protein (VSVG) inhibited with identical potency the vesicular release of VSVG from the TGN of all three cell lines. On the other hand, the VSVG peptide did not inhibit the vesicular release of HA in MDCK cells nor of two polypeptide hormones (growth hormone and prolactin) in GH3 cells, whereas in 3T3 cells (influenza) hemagglutinin was inhibited, albeit with a 3× lower potency than VSVG. The results support the existence of a basolateral-like, signal-mediated constitutive pathway from TGN to plasma membrane in all three cell types, and suggest that an apical-like pathway may be present in fibroblasts. The data support cargo protein involvement, not bulk flow, in the formation of post-TGN vesicles and predict the involvement of distinct cytosolic factors in the assembly of apical and basolateral transport vesicles.

THE TGN, a tubular *trans*-Golgi compartment (Griffiths and Simons, 1986), is the major sorting center of the secretory pathway (Griffiths et al., 1988). At the TGN, lysosomal hydrolases are sorted into clathrin-coated vesicles via mannose-6-phosphate receptors (Ludwig et al., 1995), and secretory proteins are directed into distinct populations of constitutive secretory vesicles and immature regulated secretory granules by specific sorting signals (Griffiths and Simons, 1986; Tooze and Huttner, 1990; Melancon et al., 1991). Early models postulated that plasma membrane proteins do not possess sorting signals and therefore enter by bulk flow post-TGN vesicles that transport and deliver them to the cell surface (Wieland et al., 1987). However, studies with the model viral glycoproteins influenza hemagglutinin (HA)[1] and vesicular stomatitis virus G (VSVG) proteins in MDCK cells have identified two post-TGN routes to the cell surface mediated by distinct populations of transport vesicles (Rindler et al., 1984; Wandinger-Ness et al., 1990; Rodriguez-Boulan and Powell, 1992). The existence of two post-TGN routes in epithelial cells implies that at least one of them is not a signal-blind default pathway and, indeed, transport signals have been recently identified in the cytoplasmic domain of basolateral proteins (Brewer and Roth, 1991; Hunziker et al., 1991; Le Bivic et al., 1991; Matter et al., 1992; Thomas et al., 1993). Basolateral sorting signals resemble endocytic motifs of plasma membrane receptors; thus, by analogy with the assembly of clathrin-coated vesicles, they may interact with cytosolic coat proteins that mediate the incorporation of basolateral proteins into basolateral transport vesicles (Matter and Mellman, 1994).

Address all correspondence to Dr. Enrique Rodriguez-Boulan, Department of Cell Biology, Cornell University Medical School, 1300 York Avenue, New York, NY 10021. Tel.: (212) 746-6158. Fax: (212) 746-8175.

H. Xu's present address is Laboratory of Molecular and Cellular Neuroscience, The Rockefeller University, 1230 York Avenue, New York, NY 10021.

1. *Abbreviations used in this paper*: Endo H, Endoglycosidase H; GH, growth hormone; HA, (influenza) hemagglutinin; IC-50, half-maximal inhibitory concentration; IEF, isoelectric focusing; Prl, prolactin; VSVG, vesicular stomatitis virus G protein.

In neuroendocrine cells, the basolateral protein VSVG is transported via constitutively secreted vesicles to the cell surface (Green and Shields, 1984). Exocytosis studies with chimeras of VSVG and regulated secreted proteins have shown that information for storage of regulated secretory proteins is present in the regulated secreted proteins (Moore and Kelly, 1985). It has been suggested that these sorting signals mediate packaging of proteins into immature granules by interaction with a TGN-sorting receptor (Chung et al., 1989), whereas proteins lacking appropriate signals are released via constitutive secretion by default (Moore and Kelly, 1985; Stoller and Shields, 1989). A more recent alternative hypothesis postulates that the sorting signals in regulated secretory proteins promote the formation of specific protein aggregates that exclude constitutive proteins (Chanat and Huttner, 1992). The latter are actively removed from extensions of the TGN destined to become secretory granules and from the immature granules themselves (Bauernfeind and Huttner, 1993). Evidence in support of this model is provided by kinetic studies of regulated insulin secretion in isolated pancreatic islets (Kuliawat and Arvan, 1994), by the high biochemical similarity of immature granules, condensing vesicles, and the TGN (Arvan and Castle, 1992), and by the observation of clathrin coats in immature and condensing granules (Tooze and Tooze, 1986; Orci et al., 1987*b*). As with epithelial cells, it is basic to determine whether the segregation of basolateral membrane proteins in constitutive secreting vesicles occurs by default or requires cytoplasmic sorting signals.

The observations summarized above raise fundamental questions regarding the transport of plasma membrane proteins to the cell surface of polarized and nonpolarized cells. In nonpolarized cells (*a*) are apical and basolateral proteins transported by separate post-TGN transport vesicles or by bulk flow via a single transport vesicle? (*b*) do basolateral proteins use basolateral signals and mechanisms, as in polarized MDCK cells? And in polarized cells (*c*) are basolateral signals involved in just the sorting of basolateral proteins into nascent vesicles or do they play an active role in the assembly of the vesicle?

To study the assembly of post-TGN vesicles in polarized and nonpolarized cells, we developed an in vitro assay that measures the cytosol-dependent release of apical, basolateral, and regulated secretory proteins from the TGN of semi-intact cells. The following cell lines were used: (*a*) MDCK, a polarized canine kidney line; (*b*) GH3, a rat anterior pituitary line synthesizing growth hormone (GH) and prolactin (Prl); and (*c*) 3T3, a mouse fibroblast line. To identify the characteristic basolateral route in polarized and nonpolarized cells, we studied the ability of basolateral signal peptides to compete with basolateral vesicle release. This approach is based on a recent observation by Pimplikar (1994), who showed that introduction of the 29–amino acid cytoplasmic tail of VSVG protein into perforated MDCK cells specifically blocked transport of VSVG protein from the TGN to the cell surface but did not affect that of apical influenza HA, suggesting that the peptide competed with the VSVG protein tail for a basolateral transport factor in the cytosol. This result, however, was not generalized by using other basolateral signal peptides or proteins, raising the possibility that the inhibition might have been due to an effect that is specific for the sequence of the cytoplasmic domain of VSVG and unrelated to its basolateral sorting information. Here, we studied the effect of the VSVG peptide and four other basolateral signal peptides on the release of VSVG-, HA-, GH-, or Prl-containing vesicles in the three cell lines mentioned above. Our data suggest that (*a*) the constitutive pathway of VSVG protein in 3T3 fibroblasts and GH3 cells is identical to the basolateral route in MDCK cells; (*b*) at least two post-TGN pathways to the cell surface exist in all three cell lines; and (*c*) the release of post-TGN vesicles requires the recognition of signals in cargo molecules by the transport machinery and, therefore, does not occur by bulk flow.

Materials and Methods

Cells, Viruses

MDCK II cells, passages 6–20, were grown on 10-cm plastic dishes in DME + 5% FCS. 3T3 cells, obtained from the American Tissue Culture Collection (Rockville, MD), were grown in DME + 10% FCS.

GH3 cells, a rat anterior pituitary line that secretes GH and PrL were grown in Ham's F-10 containing 2.5% FCS and 12.5% horse serum as previously described (Stoller and Shields, 1988).

Vesicular stomatitis virus, Indiana strain (VSV), and influenza virus A (WSN strain), were grown in MDCK cells as described (Rodriguez-Boulan and Sabatini, 1978).

Infection and Pulse–Chase Labeling

For viral infection, GH3 cells were inoculated with 5–10 pfu/cell, MDCK and 3T3 cells with 50 pfu/cell of wild-type VSV (Indiana strain, a gift of Dr. P. Stanley, Albert Einstein College of Medicine Bronx, NY) for 1 h at 37°C, the cells were rinsed with PBS, and incubated a further 3.5 h before radiolabeling with [^{35}S]met (New England Nuclear, Boston, MA). Mock-infected and VSV-infected cells were pulse labeled with [^{35}S]met for 10 min at 37°C followed by a chase incubation at 20°C for 2 h in the presence of 5-mM methonine and cysteine (MDCK, 3T3, GH3) and 20 μg/ml cycloheximide (MDCK, 3T3) (Stoller and Shields, 1989). MDCK and 3T3 cells were inoculated with 50 pfu/cell influenza WSN for 1 h at 37°C. Cells were then incubated for 4.5-h at 37°C and pulse labeled for 10 min with [^{35}S]cys (New England Nuclear). The chase at 20°C resulted in ~60% of the labeled VSVG/HA proteins becoming Endoglycosidase H (Endo H) resistant (see Table I). The Endo H–resistant population does not appear at the cell surface and was tested for accumulation in the TGN as described for the vesicle fractions in Fig. 1 *III*.

Vesicle Budding from Semi-Intact Cells

Permeabilized GH3 cells from control and infected cells were prepared and incubated exactly as described (Xu and Shields, 1993). The VSVG peptide (see Table II) was added directly to the assay. Pellets and supernatants of the budding assay were extracted with Triton X-100 and VSVG was immunoprecipitated with a monoclonal antibody (5FαG, kindly provided by Dr. John Lewis, SUNY Health Science Center at Brooklyn, New York). GH and Prl were precipitated with polyclonal antibodies (Xu and Shields, 1993; Austen and Shields, 1996) as described previously (Xu and Shields, 1993).

Semi-intact MDCK cells and 3T3 fibroblasts were prepared according to Beckers et al. (1987) and Xu and Shields (1993) after the reporter protein was accumulated in the TGN. In standard assays, semi-intact cells (20–25-μg protein) were suspended in a final vol of 100 μl transport buffer (Xu and Shields, 1993), supplemented with 60 or 120 μg of gel-filtered brain cytosol (conc. 20 mg/ml) (prepared according to Malhotra et al., 1989; initially kindly provided by James Rothman, Memorial Sloan Kettering Institute, New York), and energy-regenerating mix (1 mM ATP, 0.12 mM GTP, 5 mM creatine phosphate, 0.2 IU creatine kinase) and incubated for 30 min at 37°C. 120 μg cytosol was used for the initial characterization of the vesicular budding of HA and VSVG (see Figs. 1, 2, and 3). After full characterization of the cytosol dependence of the budding assay (see Fig.

5), 60 μg cytosol, the maximum concentration within the linear range, was chosen for all peptide experiments (except for Fig. 6, see legend). After incubation, samples were centrifuged for 1 min at 15,000 *g* in a microfuge, after which nascent vesicles remain in the supernatant (Xu and Shields, 1993). In the initial experiments in Fig. 1, the sedimentation of the semi-intact cells was performed by a 3-min spin at 800 *g*, conditions that gave similar results as the high-speed spin used for all later experiments. In standard assays, supernatant and pellet fractions were analyzed directly by PAGE, since viral proteins were the only labeled proteins under the infection conditions. In initial experiments (Figs. 1 and 2), VSVG and HA were immunoprecipitated after TX-100 solubilization with mAbs against the ectodomain (5FαG for VSVG, or H15-C5 hybridoma against HA, kindly provided by Dr. W. Gerhard, Wistar Institute, Philadelphia). For experiments involving immunoisolation of VSVG-containing vesicles on protein A–Sepharose beads (Fig. 1, *II c* and *e*), the supernatant fraction of a budding reaction was first incubated in high salt buffer (0.4 M KCl, 20 mM Tris/HCl, pH 8.0, for 30 min on ice) to strip peripheral proteins on the vesicles; then the salt concentration was adjusted to 150 mM KCl and immunoprecipitation of VSVG was carried out with antibodies against the cytoplasmic domain (PD4; Kreis 1986) absorbed on protein A–Sepharose (Pharmacia LKB Biotechnology Inc., Piscataway, NJ).

A chimeric protein (TGG) constituted of the ectodomain of interleukin II receptor (Tac) and cytoplasmic and transmembrane domains of the TGN38, TGG, was immuneprecipitated from transfected MDCK cells (Rajasekaran et al., 1994) with a Tac mAb (7G7; Rubin et al., 1985).

The sum of marker protein in the supernatant and pellet (S + P) fractions varied with a standard error of 3.6% (HA), 4.3% (VSVG), and 6.2% (TGG) of the total marker protein within a given experiment (see Table I for detailed analysis of this variation).

Mannosidase II was immunoprecipitated from supernatant and pellet fractions in the experiment shown in Fig. 2 after Triton X-100 solubilization using an antiserum raised against rat liver Golgi α-mannosidase II (Moremen et al., 1991) provided by Kelley Moremen, University of Georgia (Athens, GA).

For the experiments in Fig. 3, 4-μl anti-Gαs (provided by Keith Mostov, University of California at San Francisco) were pre-incubated with 50 μl cytosol for 1 h on ice. Cholera and Pertussis toxins were incubated according to Bomsel and Mostov (1993). The energy mix contained additionally, 0.1 mM GDP.

Peptide Application

HPLC-purified (>95% purity) lyophilized peptides were dissolved in water immediately before use to prevent aggregation by oxidation or denaturation. The peptides were added directly to the budding assay; their concentration was measured by UV absorbance at 205 nm after experimental determination of their extinction coefficient with the formula $E^{1mg/ml} = 27 + 120 \times A280/A205$. It should be noted that the pH of the incubation mixture was not altered by the addition of these peptides. The cytosol concentration used for all peptide experiments (60 μg) gave maximal stimulation of budding in the linear range. To determine the half-maximal inhibitory peptide concentration, the cytosol-dependent vesicle budding (after subtraction of the background budding without cytosol) in the presence of five (or four in 3T3 cells) different peptide concentrations was measured as released radioactivity in the supernatant fractions and expressed as percent of the control budding in the absence of peptide. The IC-50 values were calculated using a Cricket graph program from the slope of the linear plot of the reciprocal values of the budding (expressed as percent values) against the five peptide concentrations (Table III). The lowest correlation coefficient accepted was R = 0.75; for most graphs the correlation coefficient varied between 0.85 and 0.95. The following peptide concentrations were tested: VSVGWTp: 10, 20, 50, 100, 150 μM (for VSVG and TGG in MDCK cells); 10, 20, 50, 100, 200 μM (for HA in MDCK cells); 10, 20, 50, 150 μM (in 3T3 cells) and 10, 20, 30, 100, 150 μM (in GH3 cells); VSVGA19p: 20, 50, 100, 150, 200 μM (in MDCK cells); 10, 20, 50, 150 μM (in 3T3 cells) and 10, 20, 30, 100, 150 μM (in GH3 cells); all other peptides: 50, 100, 150, 200, 300 μM.

Digestion with Glycosidases

All digestions were performed after immunoprecipitation on protein A beads (β-galactosidase, neuraminidase) or after removing the sample from the beads by 2% SDS (Endo H) at 37°C in the presence of a protease inhibitor cocktail. After digestion, the samples were TCA precipitated and prepared for SDS-PAGE (Endo H) or digested protein was removed from the protein A–Sepharose beads by boiling in SDS gel sample buffer.

The following incubation conditions were used for the various enzymes. Endo H: 5 mU endo-β-N-acetylglucosaminidase H (Boehringer Mannheim Biochemicals, Indianapolis, IN) in 100 mM citrate buffer, pH 5.5, 0.1% SDS, for 8 h; β-Galactosidase: 1 U of jack bean meal β-galactosidase (Oxford GlycoSystems, Rosedale, NY) in 50 mM citrate buffer pH 3.5 3 × for 7 h; Neuraminidase: 5 mU Neuraminidase (Boehringer Mannheim Biochemicals) in 100 mM citrate buffer, pH 5.5, for 8 h.

Electrophoresis

SDS-PAGE. All electrophoretic procedures were carried out in 10% polyacrylamide gels according to Laemmli 1970, with the exception of the experiment shown in Fig. 1, *III e* and *f*, carried out in 8–12% gradient gels with 12% glycerol. Fluorography was carried out after impregnation of the gels in 0.1 M sodium salicylate.

Isoelectric Focusing (IEF). IEF analysis of VSVG was carried out in slab gels, 37 cm × 20 cm in size, composition 4.7% T/0.5% C acrylamide/bisacrylamide, 9.2 M urea, 2% NP-40, 1.2% ampholines, pH 5–7, 1.2% ampholines, pH 3.5–10, 0.17% ampholines, pH 7–10. The sample buffer contained 9.5% urea, 2% NP-40, 2% ampholines pH 3.5–10, 5% β-mercaptoethanol. The running time was 16 h at constant power (3 W) with maximal voltage from initial 220 V to 750 V; fluorography was carried out after impregnation with DMSO/PPO.

Quantification of Bands in Fluorograms

Gels were exposed to x-ray film for doubling time periods and the films scanned with a Mirror Scanner 800 Plus (Mirror Technologies, Inc., St. Paul, MN). Data were evaluated by measuring the amount of gray in each band above the background with the Macintosh Image 1.45 program. For the supernatant and pellet fractions, different exposures were used to ensure that the bands were in the linear range of the gray scale which was estimated by coanalyzing a standard gel with doubling amounts of radioactivity per unit area.

Electron Microscopy

Supernatant fractions of a VSVG budding reaction were pelleted in an airfuge (A100/18° rotor; Beckman Instruments Inc., Fullerton, CA) at 20 psi; the pellet resuspended and directly applied to nickel grids. Grids were contrasted with 1.5% uranyl acetate and examined in an electron microscope (100 CX; JEOL USA Inc., Peabody, MA). VSVG-containing vesicles were immunoisolated on protein A–Sepharose beads as described above, fixed in 2.5% glutaraldehyde, 0.1% Na cacodylate, pH 7.4, processed for transmission EM as previously described (Rodriguez-Boulan and Sabatini, 1978), and examined in a JEOL 100 CX electron microscope.

Results

Release of VSVG- and HA-containing Vesicles from the TGN of Permeabilized MDCK Cells

The strategy of this assay was to accumulate the basolateral reporter protein VSVG or the apical marker influenza HA protein in the TGN of MDCK cells using a reversible 20°C temperature block (Matlin and Simons, 1984) and then permeabilize the cells (Beckers et al., 1987) to study and manipulate the process of TGN-derived vesicle budding. Cells were pulse labeled for 10 min with [^{35}S]methionine/cysteine and chased for 2 h at 20°C. Under these conditions, an average of 57.5% of the nascent HA and 60.5% of VSVG accumulated in the TGN with the balance trapped in the ER and no radioactive viral protein was detectable at the cell surface. After the temperature block, permeabilized cells were prepared. We confirmed that the TGN remained intact during the preparation of semi-intact cells as antibodies against the luminal domain of TGG, a chimeric TGN marker (Humphrey et al., 1993), only stained the TGN in the presence of saponin (see Fig.

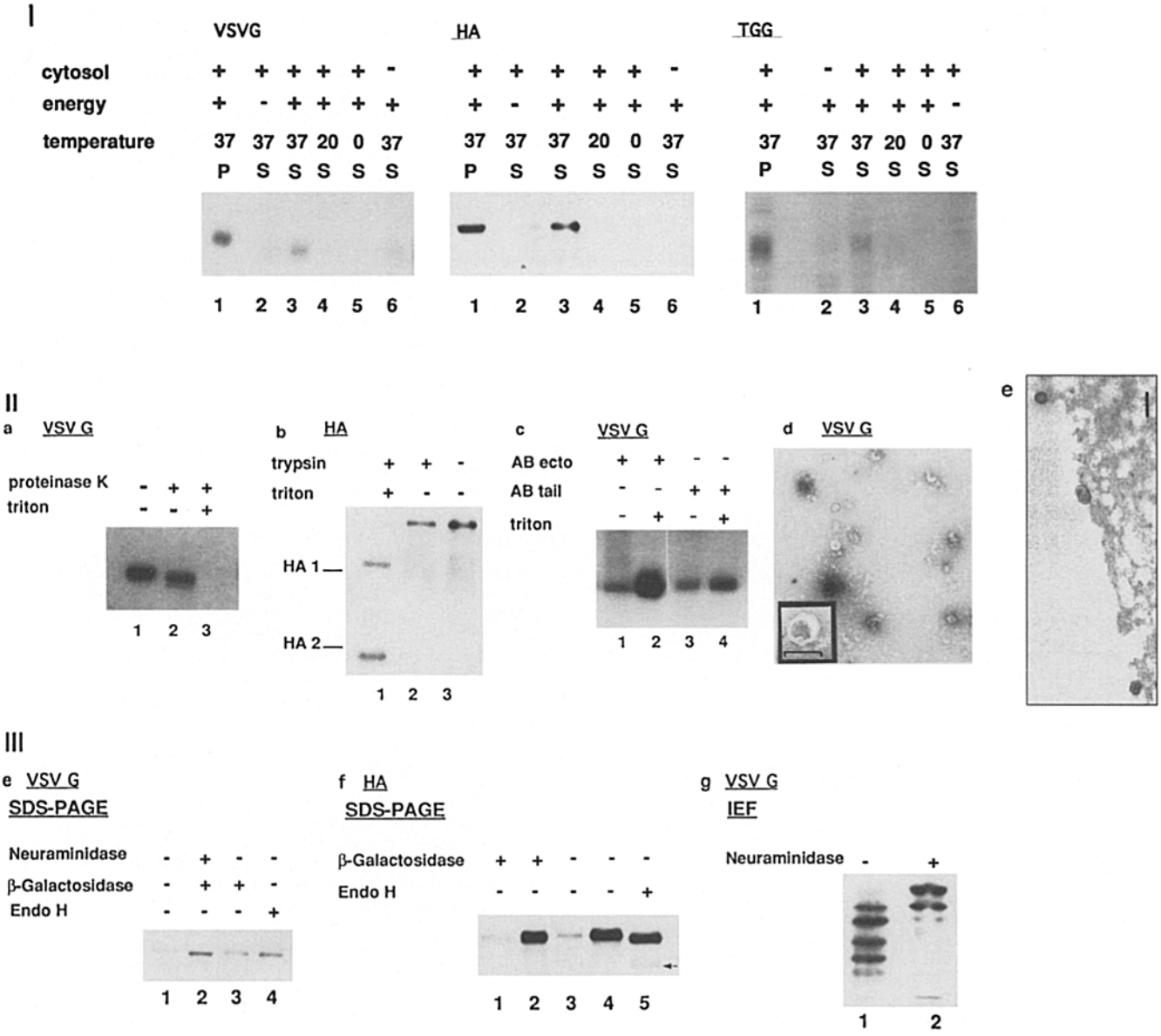

Figure 1. Release of VSVG, HA, and TGG from semi-intact MDCK cells. (*I*) Dependence on cytosol, energy mix, and an incubation temperature of 37°C. Semi-intact cells with either VSVG or HA protein accumulated in the TGN or uninfected cells expressing TGG were supplemented with gel filtrated brain cytosol and energy mix as indicated, and incubated for 30 min at 37, 20, or 0°C. The cells were sedimented and the protein in the pellet (*P*) and the supernatant (*S*) was analyzed by immunoprecipitation and PAGE; 0.6 U/ml apyrase was added to the samples in lane *2* in the VSVG and HA panel and lane *6* in the TGG panel. (*II*) The released proteins are contained in vesicles. *a* and *b*: The supernatant fraction was divided into three aliquots and proteinase K (0.5 mg/ml) or trypsin (0.5 mg/ml) and Triton X-100 (1%) were added as indicated; protease incubation occured for 30 min on ice and was inactivated by 1 mM PMSF or trypsin inhibitor. *c*: One-half of the supernatant was adjusted to 1% Triton X-100. One-half of both, the Triton-solubilized (lanes *2* and *4)* and the nonsolubilized (lanes *1* and *3*) fraction, was immunoprecipitated with antibodies against the ectodomain of VSVG (AB ecto; lanes *1* and *2*); the other half of both fractions was immunoprecipitated with antibodies against the cytoplasmic tail of VSVG (AB tail; lanes *3* and *4*). *d*: EM of negatively stained vesicles released in this assay. Bar in detail, 100 nm. *e*: Transmission EM of vesicles isolated with antibodies against the cytoplasmic domain of VSVG on protein A–Sepharose beads. Bar, 100 nm. (*III*) Vesicular VSVG and HA contain carbohydrate modifications of the late Golgi and TGN. The supernatant of a budding assay with VSVG (*e* and *g*) or HA (*f*) was immunoprecipitated and subjected to digestion with the glycosidases endo H, β-glycosidase, or neuraminidase as indicated. Neuraminidase digestion with subsequent β-galactosidase treatment was performed for sample 2 in *e*; separation of proteins occured by SDS-PAGE (*e* and *f*) or IEF (*g*); lanes *1* and *3* in *f* contain 1/20 of sample that was loaded in lanes *2*, *4*, and *5*; the arrowhead in lane *5* marks the position of the ER form of HA in the gel.

5). Furthermore, VSVG in the TGN of semi-intact cells was accessible to antibodies against the cytoplasmic domain of the protein but inaccessible to antibodies against its ectodomain (data not shown).

The addition of cytosol and an energy-regenerating system to high salt washed semi-intact cells resulted in an average of 21% of total VSVG and 27% of total HA protein (see Table I) being released into nascent vesicles, (Fig. 1 *I*

lanes *1* and *3*). In agreement with data on the formation of secretory vesicles (Xu and Shields, 1993), no VSVG or HA release was observed if the budding reaction was performed at 0 or 20°C (lanes *4* and *5*) and the release of both was decreased markedly if either cytosol or the energy-regenerating system was absent (see Fig. 1 *I* lanes *2* and *6* and Table I). The TGG chimera, which recycles efficiently between the TGN and the basolateral plasma membrane as does its endogenous counterpart TGN38 (Rajasekaran et al., 1994), was also released in a cytosol- and temperature-dependent fashion (14% in the presence versus 3.5% in the absence of cytosol), after accumulation in the TGN in the presence of cycloheximide for 2 h at 20°C (see Fig. 1 *I* and Table I).

Several experiments indicated that VSVG and HA were released into nascent vesicles (Fig. 1, *II* and *III*). (*a*) Treatment with proteinase K removed only the cytoplasmic tail of the VSVG, visible as a slight increase in its electrophoretic mobility (Fig. 1, *II a* lanes *1* and *2*). That this represented protection, but not intrinsic protease insensitivity of the ectodomain, was shown by the addition of proteinase K together with 1% Triton X-100, which resulted in complete digestion of the protein (Fig 1., *II a*, lane *3*); (*b*) antibodies against the cytoplamic tail of VSVG precipitated the protein both with and without solubilization with Triton X-100 (Fig. 1, *II c*, lanes *3* and *4*; the amount in lane *3* is 70% of that in lane *4*), whereas antibodies against the ectodomain of VSVG had access to their epitopes only when Triton X-100 was present in the immunoprecipitation reaction (Fig. 1, *II c*, lanes *1* and *2*; the amount of VSVG in lane *1* is only 18% of that in lane *2*). Isolation of VSVG membrane structures from the supernatant fraction using protein A–Sepharose beads coated with antibodies against the cytoplasmic domain of the protein revealed a population of 60–90-nm vesicles on the surface of the beads by EM (Fig. 1, *II e*). (*c*) HA has a single trypsin cleavage site in its ectodomain, giving raise to the forms HA1 (50 kD) and HA2 (25 kD). Addition of trypsin resulted in the generation of the two forms only in the presence of detergent (Fig. 1, *II b*); (*d*) the supernatant fraction of a vesicle budding assay showed a homogenous vesicle population, as determined by EM after negative staining (Fig. 1, *II d*).

To determine the origin of the vesicles carrying VSVG and HA, we analyzed the posttranslational modifications characteristic of the Golgi or TGN, using specific glycosidases (Fig. 1 *III*). VSVG protein (which possesses two complex carbohydrate side chains (Etchison et al., 1977), released into the supernatant of permeabilized cells was completely resistant to Endo H treatment, indicating that the bulk of this protein had reached the medial-Golgi complex (Fig. 1, *III e*, lane *4*) (Tarantino et al., 1978). Treatment with β-galactosidase resulted in a visible shift of the VSVG upon SDS-PAGE only when a preceding neuraminidase digestion removed the terminal sialic acid residues and rendered β-galactose the terminal residue of the complex sugars (Fig. 1, *III e*, lanes *1*, *2*, and *3*). Together with the dramatic anodic shift in the isoelectric point of VSVG protein upon neuraminidase treatment (Fig. 1, *III g*, lanes *1* and *2*), as a result of sialic acid removal, we can conclude that most of the VSVG protein had reached the TGN, the reported locale of sialyl transferases (Roth et al., 1985; Chege and Pfeffer, 1990). The mature influenza WSN HA contains, in addition to two complex carbohydrate chains, a high mannose side chain (Roth et al., 1986), and hence undergoes a large Endo H–induced electrophoretic mobility increase when it is in the ER, but only a slight mobility increase after arrival at the Golgi complex. Only a small fraction of the HA released in the supernatant underwent the large electrophoretic shift characteristic of the ER form, whereas most of the released HA was reduced only slightly in size after Endo H treatment (Fig. 1, *III f*, lane *5*). Furthermore, HA also manifested a slight shift in electrophoretic mobility upon treatment with β-galactosidase (Fig. 1, *III f*, lanes *1* and *2* versus *3* and *4*). Because it coexists with viral neuraminidase in influenza-infected cells, HA is sensitive to β-galactosidase without pretreatment with neuraminidase (not shown). These data indicated that the majority of the HA molecules had left the ER and reached at least the trans-Golgi cisternae, the postulated locale of galactosyl transferase (Kornfeld and Kornfeld, 1985).

The preceding results demonstrate that VSVG and HA released in vesicles in the TGN budding assay displayed carbohydrate modifications typical for the TGN (VSVG) or at least the late Golgi (HA). Interestingly, the population of viral glycoproteins that did not reach the TGN during the 20°C incubation period was not released efficiently

Table I. Quantitation of the Release of VSVG-, HA-, or TGG-containing vesicles from the TGN in Semi-intact MDCK Cells

	HA		VSVG		TGG	
Marker	Mean/No. experiments	Standard error	Mean/No. experiments	Standard error	Mean/No. experiments	Standard error
Percent of marker in the TGN	57.5/10	±4.1	60.5/12	±3.1	ND	
Percent budded marker (+ cytosol)	27/10	±4.2	21/12	±4.6	14/5	±5.8
Percent budded marker (− cytosol)	8/10	±2.4	3.8/12	±1.2	3.5/5	±2.1
Normalized SE of S + P	3.6/10		4.3/12		6.2/5	

The percentage of Endo H–resistant VSVG or HA protein (percent of marker in the TGN) was determined as described in Materials and Methods, after accumulation of the marker protein in the TGN by a 20°C block. The amount of each marker in the supernatant (*S*) fraction (*percent budded marker*), released in the presence or absence of 60 μg of cytosol, is expressed as a percent of the total (ER + Golgi) marker. To estimate the sample variation within individual experiments, the standard error of the sums P + S (SE_{P+S}) (where P is the amount of marker in the pellet and S is the amount of marker in the supernatant) was calculated for each experiment (5–12 samples per experiment) and normalized as a percent of the total amount of marker in the sample. In this case, mean represents the average of the normalized SE_{P+S} from *n* experiments. For example, in one of the HA experiments containing 10 samples, the values of the sums P + S were: 8,500, 8,780, 7,370, 9,010, 8,660, 7,980, 9,270, 8,370, 8,800, 9,330 pixels; therefore the mean was 8,643 pixels; the SE_{P+S} was 186.5; and the normalized SE_{P+S} was 2.15%.

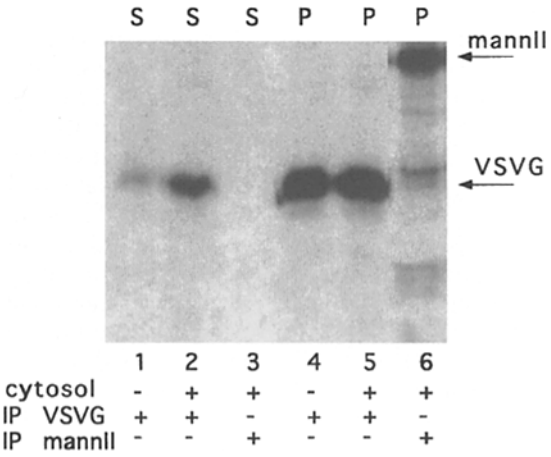

Figure 2. VSVG release is not due to fragmentation of the Golgi. MDCK cells, labeled with [^{35}S]methionine/[^{35}S]cysteine for 15 h; they were then infected with VSV, pulse labeled, and chased at 20°C as described in Materials and Methods. A standard budding assay was performed as described in Materials and Methods. One-fifth of the supernatant and pellet fractions was immunoprecipitated with antibodies against VSVG (lanes *1*, *2*, *4*, and *5*) and four-fifths of each fraction with antibodies against mannosidase II (lanes *3* and *6*). The mannosidase lanes were exposed twice as long to obtain exposures of comparable intensity to VSVG.

during the 37°C incubation in vitro, indicating that these molecules were trapped in the ER. Since an average of 21% of VSVG or 27% of HA, expressed as percent of total viral glycoprotein, was released in vesicles (Table I), and 60.5% of VSVG, or 57.5% of HA, were in the TGN (see Table I), the average vesicular release from the TGN in our standard budding assay was 35% for VSVG and 45% for HA. Although no radiolabeled protein reached the surface under the pulse-chase conditions, we excluded the possibility that VSVG-containing vesicles contained surface biotinylated plasma membrane markers (data not shown). This indicated that neither VSVG itself nor other vesicle components were derived from vesiculated plasma membrane fragments. We also excluded the possibility that VSVG was released into the supernatant fraction by artefactual fragmentation of the Golgi apparatus (Fig. 2). Immunoprecipitation of the Golgi marker mannosidase II (labeled overnight with [^{35}S]methionine/cysteine) from pellet and supernatant fractions obtained from a standard assay for VSVG release revealed undetectable levels of the enzyme under conditions where no new enzyme was produced due to host protein synthesis suppression by the virus.

Since our assay did not allow us to determine directly if HA and VSVG protein were released into distinct apical and basolateral vesicles distinguished by their ability to fuse with the appropriate surface domains, we investigated pharmacologic features of TGN vesicle budding that may discriminate between HA- and VSVG-containing vesicles.

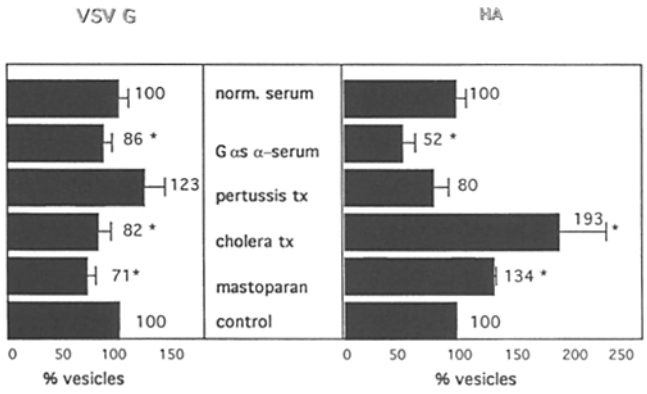

Figure 3. The budding of VSVG and HA are differentially effected by stimulators or inhibitors of trimeric G proteins. Budding assays for VSVG and HA (as in Fig. 1 *I*) were performed in the presence of 10 μM Mastoparan, 100 μg/ml Cholera or Pertussis toxins or anti-Gαs serum or normal serum as described in Materials and Methods; budding as percentage of control samples was determined in three or four experiments. *, a significant difference for HA and VSVG ($P \leq 0.05$), determined by a paired *t* test.

Pimplikar and Simons (1993) have suggested that different trimeric G proteins regulate transport of apical and basolateral proteins from the TGN to the cell surface with Gαi being a negative regulator for basolateral transport and Gαs a positive regulator of apical transport. We therefore determined if this regulation could occur at the level of vesicle release from the TGN. Cholera toxin, an activator of Gαs, stimulated HA protein budding almost two-fold, whereas pertussis toxin, an inhibitor of Gαi stimulated VSVG protein budding and slightly inhibited that of HA (Fig. 3). Consistent with this observation, antibodies against Gαs inhibited predominantly the release of the apical marker, and mastoparan, which is known to mimic receptors for Gαi, inhibited release of the basolateral protein from the TGN (Fig. 3). When expressed as percentage of controls, vesicular budding of VSVG and HA were significantly different from each other in the presence of mastoparan, cholera toxin, and Gαs antibodies, suggesting that VSVG and HA are released into different vesicle types. The data further indicate that the regulation of TGN to surface transport of VSVG and HA by trimeric G proteins occurs at the level of vesicle release from the TGN, suggesting that Gαi and Gαs may interact with membrane proteins that are part of the basolateral and apical vesicle transport machinery at the TGN.

Effect of Peptides Possessing Basolateral Targeting Domains on the Budding of Basolateral and Apical Proteins from the TGN

If the cytoplasmic tails of basolaterally targeted proteins interact with cytosolic factors, it should be possible to interfere with this process by adding appropriate peptides to the in vitro budding assay. The peptides tested (VSVGp,

Figure 4. The effect of VSVG and VAVGA19 peptides on the budding of VSVG and HA protein in MDCK and 3T3 cells. (*A*) A peptide representing the 29-aa long cytoplasmic domain of VSVG protein (*VSVG*) or a control peptide where Alanine was exchanged for Tyr19 (VSVGA19) were incubated at the indicated concentrations with 3 μl (60 μg) cytosol in the VSVG or HA protein budding reaction in MDCK (*top*) or 3T3 cells (*bottom*). TGG protein release in the presence of VSVGp and VSVGA19p was studied in uninfected

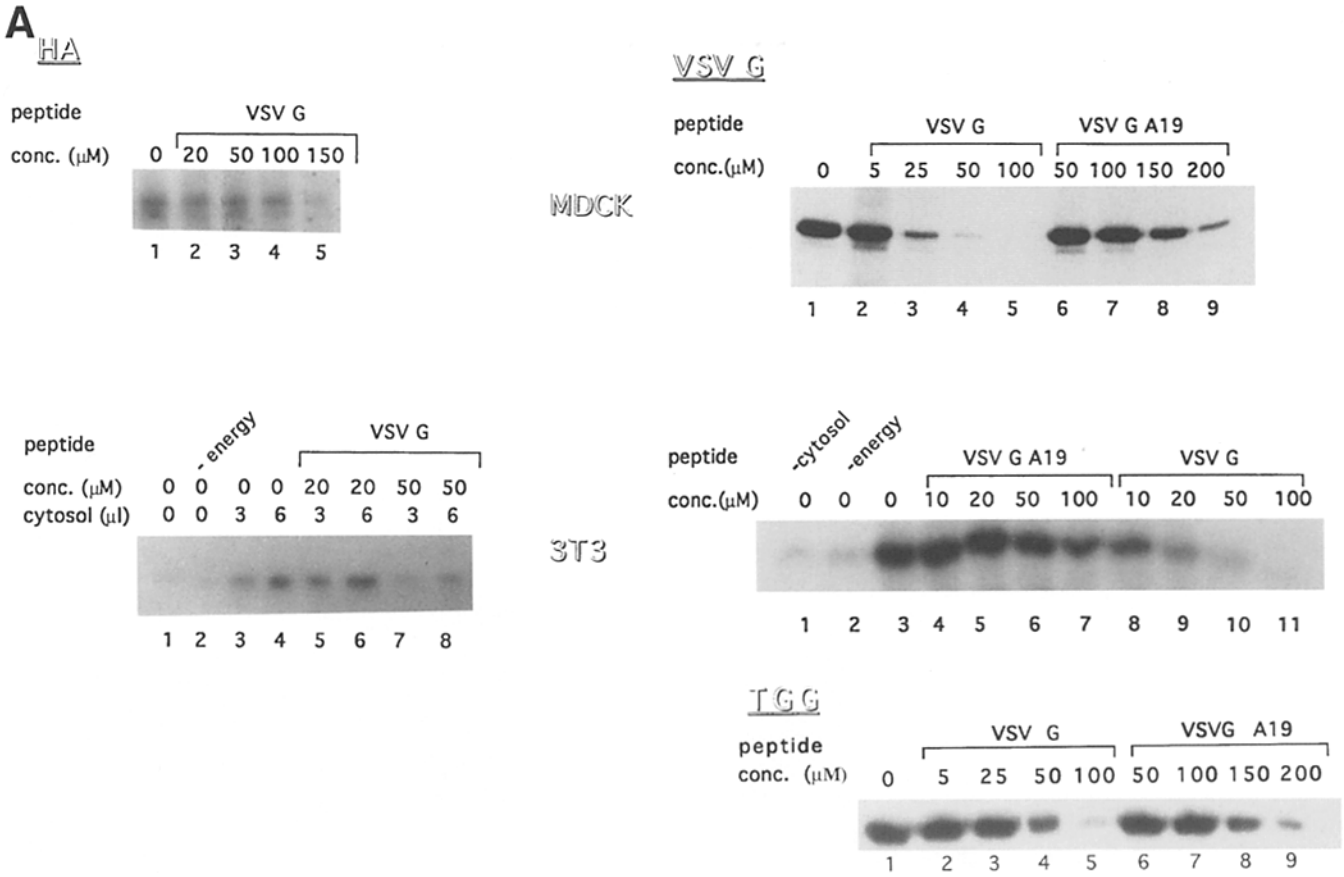

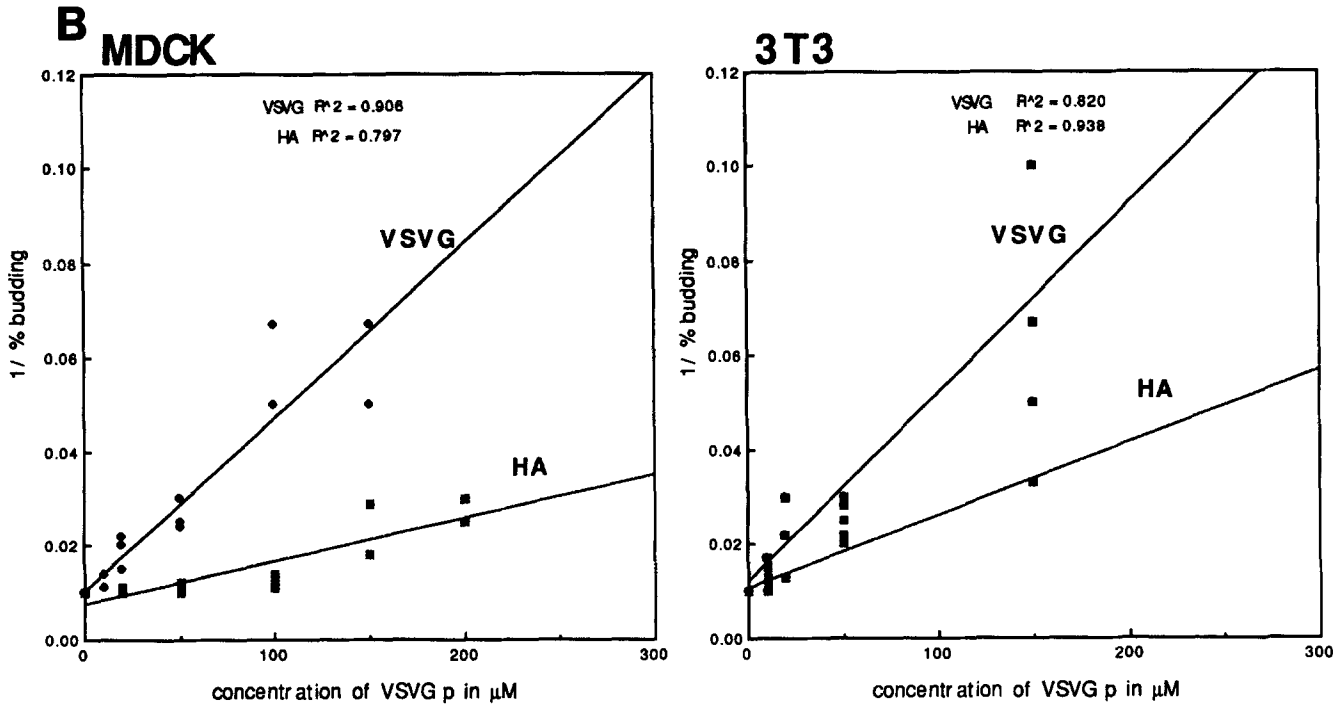

MDCK cells expressing the TGG marker. The gels show vesicular VSVG, HA, or TGG protein in the supernatant fractions. For assays in 3T3 cells, cytosol and energy dependence of vesicle release is shown(-cytosol, -energy). The HA-budding assay was supplemented with 3 and 6 μl cytosol. *(B)* The reciprocal values of VSVG and HA budding, expressed as percentage from controls, were plotted against the concentration of VSVGp in a linear plot with correlation coefficients between 0.797 and 0.938 using the Cricket graph program. The data points represented were from three experiments using five (MDCK) or four (3T3) concentrations of VSVGp for each experiment. The IC_{50} was calculated from the slope of the graphs. For details see Materials and Methods.

Table II. Peptides Tested on the Budding of VSVG-containing Vesicles from the TGN

Peptide	Protein	From TGN to:	Final appearance at:	Peptide sequence	Evidence for sorting information	Ref.
pIgR	pIg receptor	bl PM	ap PM	R-A-R-H-R-R-N-V-D-R-V-S-S-I-G-S-Y-R	Deletion mutants are targeted apically. Peptide redirects a recombinant apical protein (PLAP)	* ‡
LEP 100	Lysosomal associated protein	bl PM or endosome	lysosome	K-S-H-A-G-Y-Q-T-I		§
TGN38		bl PM	TGN	R-R-P-K-A-S-D-Y-Q-R-L-N-L-K-L	15 COOH-terminal aa; deletions result in nonpolarized or apical surface distribution	‖
VSVG		PM	bl PM	R-V-G-I-H-L-C-I-K-H-T-K-K-R-Q-I-Y-T-D-I-E-M-N-R-L-G-K	Complete cytoplasmic tail contains basolateral sorting information	‡‡
VSVGA19	Mutant of VSVG (Y19 to A19 in the cytoplasmic tail)	ap PM	ap PM	R-V-G-I-H-L-C-I-K-L-H-T-K-K-R-Q-I-A-T-D-I-E-M-N-R-L-G-K	Cytoplasmic tail with Y to A mutation causes apical polarity of the mutant protein	‡‡
HAY	Mutant of hemagglutinin (C7 to Y in the cytoplasmic tail)	bl PM	bl PM	K-N-G-S-L-Q-Y-R-I-C-I	C7-Y point mutation changes targeting of the apically targeted wildtype protein	
HAC	Hemagglutinin	ap PM	ap PM	K-N-G-S-L-Q-C-R-I-C-I		¶
LDLCT12	Deletion mutant of LDL receptor	ap PM	ap PM	K-N-W-R-L-K-N-I-N-S-I-N		**
1gp120C8	Y8 to C8 mutant in the cytoplasmic tail	ap PM	ap PM	R-K-R-R-H-A-G-C-Q-T-I	Mutant protein stays at the apical surface instead of going to the lysosome via the basolateral surface	**
R1	Somatostatin 28 (1–14)	–	–	S-A-N-S-N-P-A-M-A-P-R-E-R-K	Irrelevant peptide	
R2	Fibrinogen related protein	–	–	G-Q-Q-H-H-L-G-G-A-K-Q-A-G-D-V	Irrelevant peptide	
R3	Folicular gonadotropin releasing peptide	–	–	T-D-T-S-H-H-D-Q-H-P-T-F-N	Irrelevant peptide	

*Mostov et al., 1987; †Casanova et al., 1991; §Nabi et al., 1991; ‖Rajasekaran et al., 1994; ¶Thomas et al., 1993; **Brewer and Roth, 1991; ‡‡Matter et al., 1992; bl = basolateral, ap = apical, PM = plasma membrane.

HAYp, TGN 38p, LEP100p, pIgRp) and the evidence for their basolateral sorting information is shown in Table II. Three arbitrarily chosen peptides (R1, R2, R3) and three peptides representing the entire cytoplasmic tail of apically targeted proteins (HAC, lgp120C8, LDLCT12) served as controls for these experiments. The most potent inhibitor of VSVG vesicle budding was VSVGp, a peptide corresponding to the 29 cytoplasmic amino acids of VSVG, which contains a well-established basolateral signal (Thomas et al., 1993). VSVGp inhibited budding of VSVG-containing vesicles at 25 μM and caused almost complete inhibition at ~50 μM (Fig. 4 *A*). In contrast, a mutant peptide that fails to act as a basolateral signal in vivo (Thomas et al., 1993), VSVGA19p, was approximately six times less efficient as an inhibitor in the in vitro assay (IC50 = 24 μM vs. 143 μM, respectively, Table III). Furthermore, VSVGp was approximately six times less efficient in inhibiting the budding of influenza HA from the TGN of MDCK cells, indicating a strong preference for the basolateral mechanism (Fig. 4 *A*, VSVG vs. HA, *top*).

Since the mutant VSVGp had little effect on vesicle budding and the wild-type peptide had dramatically different effects on VSVG and HA release, this attested to the specificity of the budding of VSVG-containing vesicles from the TGN. To exclude further the posssibility that VSVGp did not cause disruption of the Golgi, we demonstrated that TGG remained inaccessible to antibodies in the presence of 50 μM VSVGp in semi-intact cells and that at the EM level, the appearance of Golgi stacks was not altered (Fig. 5).

We considered the possibility that the inhibitory effect of VSVG peptide on the release of VSVG protein was due to identity between the peptide and the protein being transported. To exclude this possibility, we studied the effect of VSVGp on a second basolateral marker, TGG. VSVGp inhibited the budding of vesicles carrying TGG with an IC-50 ~43 μM, even lower than the IC-50 of the homologous peptide TGN38p (see Table III and Fig. 4 *A*, TGG panel). Our data therefore demonstrate that the potent inhibitory effect of VSVGp on the release of basolateral vesicles in general reflects a functional property of the basolateral vesicle budding system.

Two other peptides, HAYp and TGN38p, inhibited the budding of VSVG vesicles at higher concentrations (IC-50 ~115 and ~83 μM) than VSVGp. The control peptides (HAC, LDLCT12, R1, R2, R3), however, were ineffective at these concentrations (Tables II and III). HACp, representing the cytoplasmic domain of wild-type HA, had a considerably reduced inhibitory potency compared with HAYp from which it differs only in a single amino acid. The inhibitory effect of the HAY peptide was dependent on the same tyrosine residues that are critical for basolateral targeting in vivo (Brewer and Roth, 1991; Thomas et al., 1993). Therefore, HACp provides a strong argument for the validity of our assay as tool to characterize the basolateral sorting mechanism. Our results generalize previous observations by Pimplikar et al. (1994) showing that the VSVG peptide inhibits specifically not only the exit of VSVG protein from the TGN but also, and with high potency, the release of a second basolateral marker, TGG, and by demonstrating that other basolateral signal peptides (HAYp, TGN38p) inhibit the release of VSVG protein. As with VSVGp, the inhibitory effect of HAY was highly specific since the release of the basolateral marker was dependent on a crucial tyrosine residue necessary for basolateral targeting in vivo.

The inhibitory effect of the basolateral signal peptides may be due to their competition with a cytosolic factor for the binding to VSVG. If this were the case it should be possible to overcome the inhibitory effect of the peptides by increasing the amount of cytosol in the budding assay. Fig. 6 shows that this is the case for the VSVGp. Fig. 7 (*left*) indicates that the inhibitory effect of TGN38p and HAYp could also be overcome by increasing amounts of cytosol.

As mentioned above, VSVGp did not interfere with the budding of vesicles carrying HA at concentrations that completely blocked the budding of VSVG vesicles (Fig. 4 *A*). This result favors our interpretation that VSVGp specifically interferes with the release of basolateral transport vesicles in polarized MDCK cells. On the other hand, the three peptides VSVGp, HAYp, and TGN38p inhibited the vesicular release of HA with IC-50's of ~150 μM. In contrast, the control peptide HAC had an effect on the vesicular release of HA only at a concentration of 300 μM (Ta-

Table III. Peptide Concentrations that Cause Half-Maximal Inhibition of the Release of VSVG-, TGG-, or HA-containing Vesicles from the TGN in MDCK and 3T3 Cells

	MDCK cells			3T3 cells	
Peptide/protein	VSVG	TGG	HA	VSVG	HA
LEP100	330 μM ± 100 (3)				
pIgR	> 300 μM (3)				
HAY	115 μM ± 35 (3)		150 μM ± 15 (3)		
TGN38	83 μM ± 10 (3)	120 μM (2)	160 μM ± 22 (3)		
VSVG	24 μM ± 4 (3)	43 μM (2)	145 μM ± 22 (3)	20 μM ± 4 (3)	60 μM ± 10 (3)
VSVGA19	143 μM ± 5 (3)	140 μM (1)	160 μM ± 45 (3)	134 μM ± 9 (3)	
HAC	> 300 μM (3)		320 μM ± 37 (3)		
LDLCT12	>300 μM (3)				
Igp120C8	> 300 μM (3)				
R1	> 300 μM (2)				
R2	> 300 μM (2)				
R3	> 300 μM (2)				

Vesicle budding assays for VSG, TGG, or HA protein were performed in the absence or presence of the listed peptides. Vesicle budding in the presence of peptides was expressed as percentage of control budding in the assay without peptide and its reciprocal values were plotted against the peptide concentrations. The 50% inhibitory concentration and the standard deviation were calculated from the number of experiments indicated in brackets for each peptide as described in Materials and Methods.

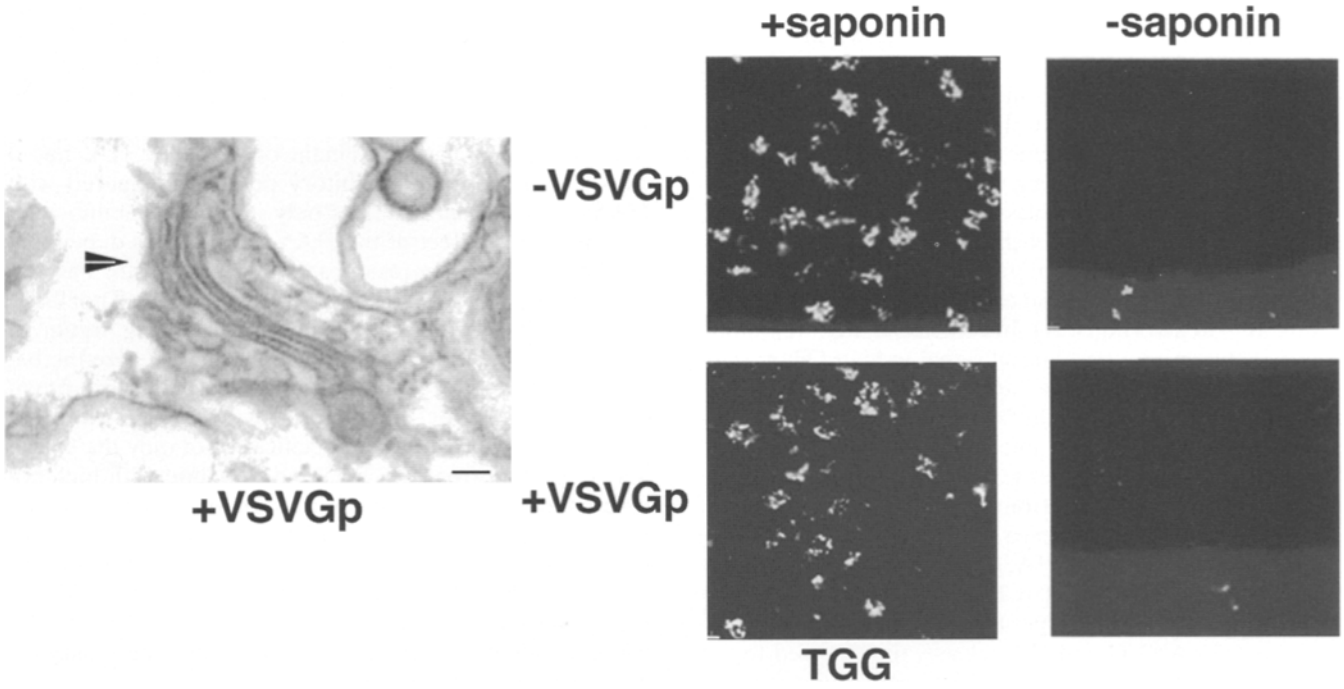

Figure 5. The VSVG peptide does not disrupt Golgi structure. A standard budding assay was carried out with semi-intact MDCK cells permanently transfected with TGG in the presence or absence of 50 μM VSVGp. Aliquots of the pellet fractions were fixed with 2% paraformaldehyde and processed for immunofluorescence with antibodies against the ectodomain of the TGN marker TGG (*Tac*) in the presence or absence of 0.075% saponin. The labeled semi-intact cells were spread on coverslips, mounted on glass slides, and analyzed by confocal microscopy. Another aliquot of the pellet was fixed in 2% glutaraldehyde, 0.1 M cacodylate buffer, pH 7.4, and processed for transmission EM. Note that the addition of the peptide did not increase the accessibility of the luminal Tac epitopes to antibodies nor abolished the stacked organization of the Golgi.

ble III). The inhibitory effect of the three signal peptides was reduced in the presence of higher cytosol concentrations in the assay (Fig. 7, *right*), suggesting that the effect of the peptides on the HA vesicle budding was due to a competition with soluble factors that are similar or identical with basolateral transport factors. Note that whereas 3 μg/ml cytosol partially overcame the inhibition of HA release by 150 μM VSVGp, it did not overcome the inhibition of VSVG release by 50 μM VSVGp, a result that further underlines the differential inhibitory effect of VSVGp on basolateral vs. apical vesicle release.

Effect of VSVGp on the Budding of VSVG or HA Vesicles from the TGN in 3T3 Cells

Since the VSVG peptide allowed us to discriminate between the pathways for apical and basolateral vesicle release from the TGN in MDCK cells, this peptide was used to study whether VSVG protein and HA are released in a single vesicle type or in different vesicles from the TGN of nonpolarized fibroblasts. Permeabilized 3T3 cells with either VSVG or HA protein accumulated at the TGN were prepared. Omission of cytosol or the energy mix reduced the vesicular marker protein in the supernatant to 20% (Fig. 4 *A*, *3T3* panel, see lanes *1* and *2*). VSVGp and VSVGA19p inhibited the budding of VSVG-containing vesicles with IC-50 ~20 and 134 μM, respectively (Table III, Fig. 4 *A*), identical to those in MDCK cells, indicating that a pathway corresponding to the basolateral route in MDCK cells exists in 3T3 fibroblasts and has a similar transport capacity as in the epithelial cell line. The release of HA from the TGN of 3T3 cells was inhibited by the VSVG peptide with a IC-50 of 60 μM (Fig. 4, Table III). This represents an inhibitory potency 3× lower than for VSVG, suggesting that a population of HA molecules is transported via a peptide-insensitive pathway. Fig. 4, however, also shows that the peptide inhibited the release of HA protein in 3T3 cells with a 2.5× higher inhibitory potency than in MDCK cells. Furthermore, whereas 50 μM VSVGp caused no inhibition of HA budding in the presence of 3 μl cytosol, the same peptide concentration reduced HA budding in 3T3 cells by ~50%, even in the presence of 6 μl cytosol in the budding assay. Higher cytosol concentrations, however, were effective in overcoming the effect of 50 μM peptide in this cell line as expected for an interaction between the peptide and a cytosolic factor (data not shown). The observation that the inhibitory potency of the VSVG peptide on the release of HA protein in 3T3 cells was intermediate between its poor inhibitory potency on HA protein budding in MDCK cells and its powerful effect on VSVG protein release in both cell lines suggests that an apical-like pathway exists in 3T3 fibroblasts, albeit with a lower capacity than in MDCK cells.

Budding of VSVG-containing Vesicles and Nascent Secretory Granules in Permeabilized GH3 Cells

Earlier work (Green and Shields, 1984) suggested that GH and VSVG protein are sorted into different vesicle populations in VSV-infected GH3 cells. This sorting step was presumed to occur late in the secretory pathway because inhibition of GH secretion had no effect on the appear-

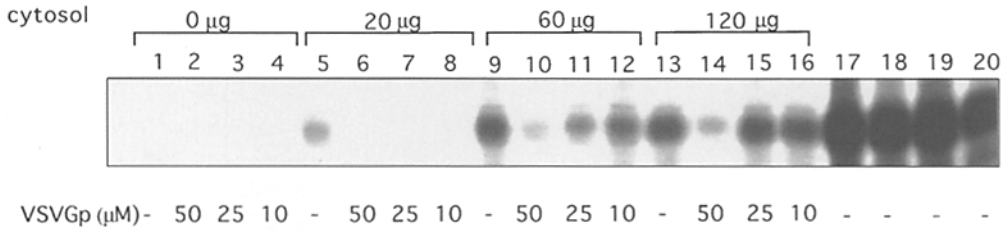

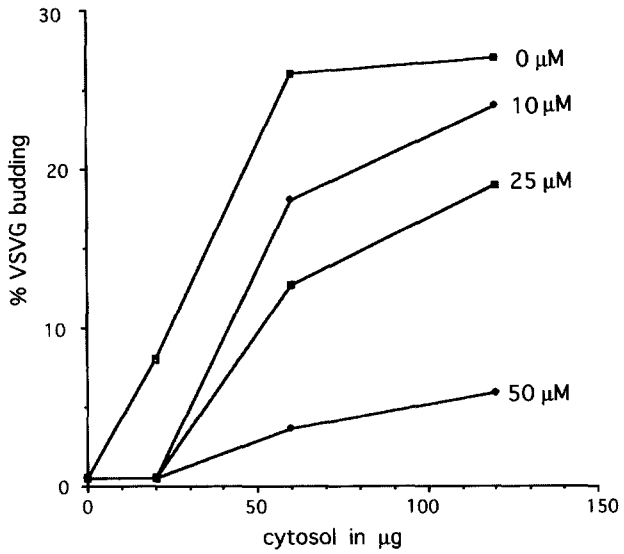

Figure 6. The inhibitory effect of VSVGp is dependent on the cytosol concentration in the budding assay. VSVG vesicle budding assays were performed in the presence or absence of 10, 25, or 50 μM VSVGp supplemented with 0, 20, 60, or 120 μg cytosol. Supernatant and pellet fractions were analyzed as described in Materials and Methods and the percentage of total VSVG released into the vesicle fraction was plotted against the cytosol concentrations. Lanes *1–16* are supernatant fractions; lanes *17–20* are the pellet fractions corresponding to control samples (no peptide added; lanes *1*, *5*, *9*, and *13*, respectively).

ance of VSVG protein at the plasma membrane or on virus assembly. Based on the preceding data and these earlier observations, we hypothesized that the VSVG peptide would interfere with VSVG protein vesicle budding, but would have little effect on the formation of GH- or Prl-containing secretory vesicles. To test this idea, we prepared permeabilized cells from VSV-infected GH3 cells (Xu and Shields, 1993) and added either VSVG peptide or the VSVGA19 control peptide to the in vitro budding system (Fig. 8). Consistent with our earlier observations, vesicle budding from the TGN was energy and cytosol dependent (Fig. 8 *A*, compare lanes *12* and *13* with *25* and *26*). Addition of the VSVG peptide to the permeabilized cells inhibited vesicle budding fourfold at a concentration of 20–30 μM (Fig. 5 *A*, lanes *3*, *4*, *16* and *17*; *D*). In agreement with the preceding data on MDCK cells, the mutant VSVG A19 peptide had no effect on vesicle formation even up 150 μM (Fig. 8 *A*, lanes *7–12* and *20–24*; *D*). In contrast, addition of the VSVG peptide had no effect on the budding of either GH- or Prl-containing nascent vesicles (Fig. 8 *B* and *C*, respectively, Fig. 6 *E*). It should be noted that in *B* and *C*, the permeabilized cell system was prepared from uninfected cells because VSV infection completely inhibits endogenous GH and Prl synthesis and in this case vesicle budding did not require addition of cytosol.

In agreement with our earlier observations, these results strongly suggest that VSVG protein is packaged into a different population of vesicles from those containing either GH or Prl. Most significantly, the current data imply that the host cell "target" molecules that interact with the cytoplasmic tail of VSVG protein to effect its packaging into vesicles, can be inhibited without affecting formation of nascent secretory granules.

Discussion

A main goal of this work was to study the requirement of basolateral sorting signals in the constitutive transport of VSVG protein to the surface of polarized and nonpolarized cells. Basolateral sorting signals have been identified unequivocally in the cytoplasmic domain of a variety of basolateral proteins (Matter and Mellman, 1994), but their role in anterograde transport is not well understood. We wished to determine whether (*a*) nonpolarized cells require signals to transport basolateral proteins from the TGN to the cell surface or, alternatively, use a default mechanism, as widely believed (Alberts et al., 1994); (*b*) basolateral signals act by concentrating and sorting basolateral proteins into nascent basolateral vesicles or by promoting the assembly of the basolateral vesicles themselves; (*c*) cytoplasmic signals are required to segregate VSVG protein from regulated secretory proteins. To this end we used different permeabilized cells, incubated in the presence and absence of basolateral signal peptides, and compared the release of the VSVG protein from the TGN with that of several proteins whose intracellular transport is diagnostic for different vesicle populations (Figs. 4 and 8, Table III).

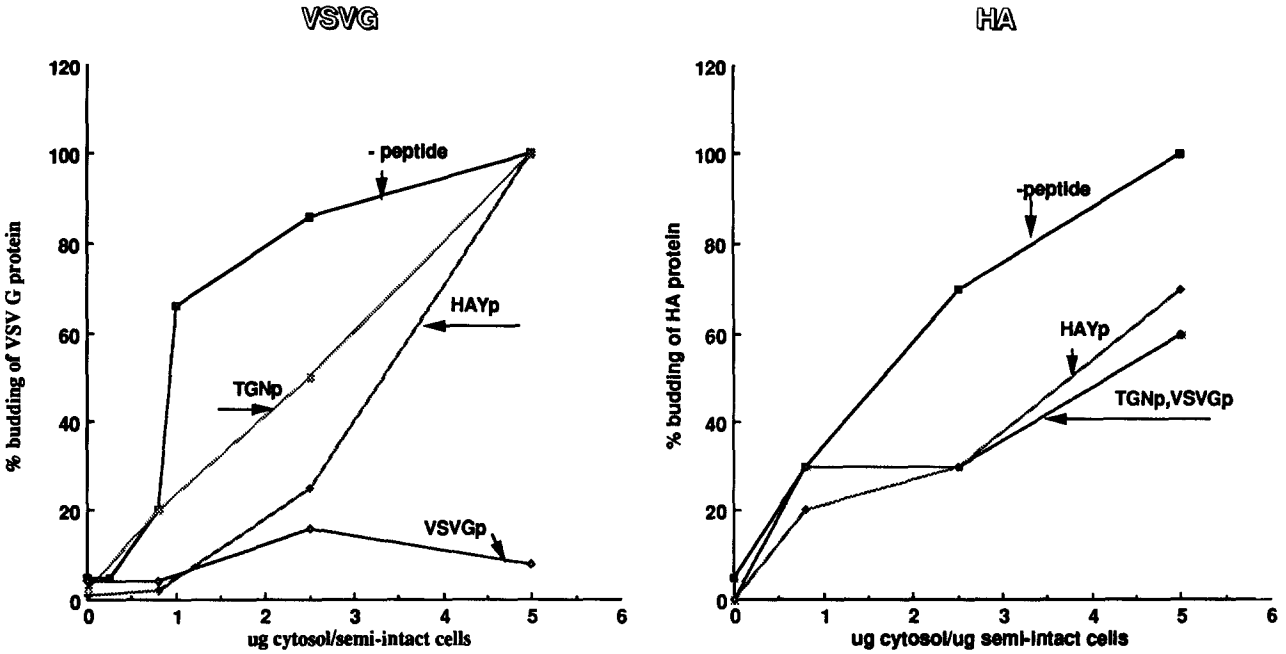

Figure 7. VSVGp inhibits differentially the release of VSVG protein over HA whereas HAYp and TGN 38p inhibit HA and VSVG release to the same extent in a cytosol-dependent manner. Vesicle budding of either VSVG or HA protein was assayed in the presence or absence of one of the following peptides: 150 μM TGN38p, 150 μM HAYp (VSVG and HA protein), 50 μM VSVGp (for VSVG protein) or 150 μM VSVGp (for HA protein). The cytosol concentrations in the assay were 0.75 mg/ml, 1.5 mg/ml–3 mg/ml with a constant concentration of semi-intact cell protein of 0.6 mg/ml. Values for vesicle budding are expressed as percentage of the highest amount of vesicular VSVG or HA protein released into the supernatant. Data points are the average of two experiments.

Transport of VSVG Protein Requires a Cytoplasmic Signal in Nonpolarized Cells

The requirement for signals in anterograde transport from the TGN might have evolved in epithelial cells as a consequence of their need to target proteins to two different surface domains. If so, it might be expected that a basolateral signal peptide would not inhibit transport of a basolateral protein in nonpolarized cells, where proteins would follow a bulk flow pathway to the cell surface. However, the VSVG peptide inhibited the release of VSVG with the same potency in 3T3 cells as in MDCK cells (IC-50 ~20–25 μM), indicating that VSVG, a prototype marker for bulk flow studies (Moore and Kelly, 1985; Orci et al., 1986; Wieland et al., 1987) requires cytoplasmic signals to exit the TGN of nonpolarized and polarized cells (Fig. 4). The strict signal dependence of VSVG tranport in nonpolarized cells suggests that proteins not possessing these signals, e.g., apical proteins, might use a separate transport mechanism, equivalent to the apical transport pathway of epithelial cells. Since the release of influenza HA from the TGN of MDCK cells could be distinguished by its 6× lower sensitivity to VSVGp (IC-50 ~145 μM) we tested the effect of VSVGp on the release of influenza HA in 3T3 fibroblasts. We found that VSVGp inhibited release of the apical marker HA in 3T3 fibroblasts with an intermediate potency (apparent IC-50 ~60 μM) between VSVG (20 μM) and HA (IC-50 ~145 μM) in MDCK cells. Because the budding of HA vesicles is more sensitive to VSVG peptide in 3T3 cells than in MDCK cells, we suggest that the machinery to generate apical vesicles may be present but not fully developed in these nonpolarized fibroblasts. In fact, the capacity of the apical transport pathway appears to be highly variable even in epithelial cells; in intestinal cells it appears to be underdeveloped, whereas it is absent in hepatocytes (for reviews see Rodriguez-Boulan and Powell, 1992; Matter and Mellman, 1994).

Role of Basolateral Signals in the Assembly of Basolateral Vesicles

Our in vitro data do not support the bulk flow model of protein transport to the plasma membrane, which suggests that Golgi-derived transport vesicles are constantly formed independently of the presence or absence of signals in the cargo protein. In our experiments, the VSVG protein is the major cargo protein in the TGN because host cell protein synthesis was inhibited by viral infection. The complete inhibition of VSVG release by VSVGp suggests that VSVG cannot be transported by an alternative apical route in the absence of apical cargo proteins. This contrasts starkly with the in vivo observation in transfected cells, that VSVG protein is missorted but not blocked by the inactivation of its basolateral signal by mutagenesis (Rose and Bergmann, 1983; Gonzalez et al., 1987; Thomas et al., 1993). In fact, the observation that VSVGp is twofold less efficient in inhibiting the release of TGG-containing vesicles in noninfected cells could be also explained by the existence of an apical transport pathway in these cells. Our results lead us to conclude that (*a*) the release of basolateral proteins in transport vesicles requires the interaction of cargo protein sorting signals in the TGN with a component of the transport machinery in the TGN and hence does not occur by bulk flow, and (*b*) apical vesicles

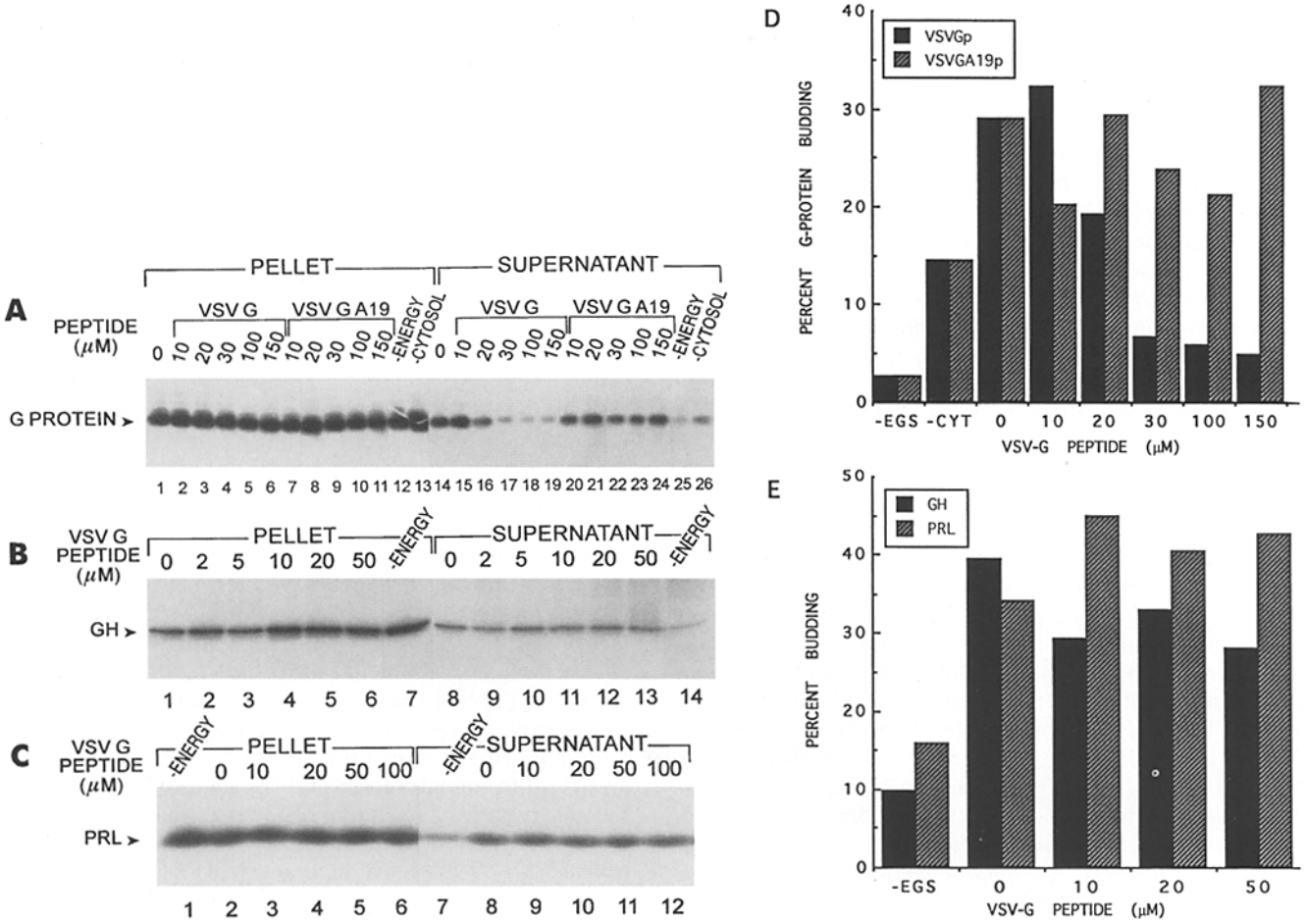

Figure 8. Effect of VSVG and VSVGA19 peptides on the budding of VSVG and growth hormone or prolactin in GH3 cells. VSV- (*A*) or mock-infected (*B* and *C*) permeabilized GH3 cells were incubated with cytosol and energy mix to release TGN-derived vesicles. VSVG peptide or the control peptide VSVGA19 was incubated at the indicated concentrations with the cytosol in budding reaction; both, the vesicle fraction (*SUPERNATANT*) and the semi-intact cells (*PELLET*) were immunoprecipitated with anti-VSVG (*A*), anti-GH (*B*), or anti-Prl (*C*) antibodies; -CYTOSOL and -ENERGY indicate that either cytosol or the energy-regenerating system was omitted in the assay. (*D* and *E*) The intensities of each band were quantitated using a computing densitometer (300A; Molecular Dynamics Inc., Sunnyvale, CA). Budding efficiency (percent budding) = (sum of the band intensities from the supernatant [vesicle fraction]) ÷ (sum of the band intensities from the pellet and supernatant) × 100.

are not released by bulk flow, since a basolateral protein can be missorted into apical vesicles only when apical cargo proteins are present in the TGN but not in their absence. A corollary is that basolateral proteins can use an existing apical pathway but cannot create one.

Our experimental conditions did not allow us to test directly whether the cytoplasmic domain of VSVG protein is necessary just to concentrate VSVG into post-TGN transport vesicles or, alternatively, is necessary for the assembly of the vesicles. In the first scenario, addition of VSVG peptide would result in the production of "empty" transport vesicles, whereas in the second scenario no post-TGN basolateral vesicles would be formed in the presence of VSVGp. We favor the second possibility based on the in vivo data described above. 50–67% VSVG protein carrying an inactivated basolateral sorting signal is transported efficiently to the basolateral surface of transfected MDCK cells (Gonzalez et al., 1987; Thomas et al., 1993), where other basolateral proteins are synthesized and delivered to the cell surface, suggesting that VSVG protein is included in basolateral transport vesicles as long as other basolateral proteins promote the assembly of these vesicles. Hence, lack of sorting can not result in complete inhibition of transport. Rather, the complete inhibition of transport observed in infected cells exposed to VSVG peptide (Pimplikar and Simons, 1994; and this paper) most likely reflects the complete inhibition of vesicle release from the TGN.

A surprising outcome of our study was the similar inhibitory potency of the basolateral sorting peptides HAYp and TGN38p on the release of basolateral and apical vesicles in MDCK cells. We suggest that this effect is due to the basolateral signal content in both peptides for two reasons: (*a*) the control HAC peptide (the normal cytoplasmic domain of influenza HA which has no activity as a basolateral signal), did not inhibit the budding of either marker; (*b*) none of the other tested nonsignal peptides inhibited the release of either marker at similar concentrations. Recent evidence indicates that signals for coated pit, TGN, and lysosomal localization share structural features with basolateral signals (Thomas and Roth, 1994). The

short peptides HAYp and TGN38p could represent degenerate signals sufficient to be recognized by both apical and basolateral soluble binding factors; only the VSVG peptide, with 29 amino acids by far the longest peptide tested, could meet the requirements for a basolateral sorting sequence strictly, resulting in a six times higher inhibitory potency for basolateral vesicles (IC_{50} ~24 μM) than for apical vesicles (IC_{50} ~145 μM). These results further suggest that the exit of apical proteins from the TGN of MDCK cells also requires specific cytoplasmic factors. Since apical membrane proteins do not seem to contain cytoplasmic targeting information, or simply lack cytoplasmic domains, the signal for assembly of apical vesicles would be contained in a transmembrane apical sorting receptor. This receptor could function as an adaptor by interacting with apical markers via its luminal domain and with the vesicle assembly machinery via its cytoplasmic domain. Alternatively, HAYp and TGN38p could bind a different soluble budding factor than VSVGp, one that is involved in the production of both apical and basolateral vesicles.

An unexpected observation was that two basolateral signal peptides, LEP100p and pIgRp, did not inhibit the release of the basolateral marker VSVG. Two possible scenarios can be envisioned that would explain this observation. An interesting possibility is that their failure to inhibit the release of VSVG-containing vesicles from the TGN may reflect the use of alternate basolateral targeting mechanisms by pIgA-R and LEP-100. In fact, in contrast to VSVG, pIgA-R is rapidly endocytosed and undergoes a second sorting event in basolateral endosomes (Aroeti and Mostov, 1994). Furthermore, pharmacological studies using brefeldin A have suggested that pIgA-R might use a pathway to the plasma membrane different from other basolateral proteins (Apodaca et al., 1993). An alternative trivial explanation of the data is that the pIgA-R and LEP-100 peptides fail to adopt the competent secondary structure they have in the context of the protein from which they are derived. However, the pIgA-R peptide functions as a basolateral sorting signal when transferred to other proteins (Casanova et al., 1991) and alters its secondary structure in solution when signal-disabling mutations are introduced, as determined by NMR analysis (Aroeti et al., 1993), suggesting that it may preserve basolateral signal activity in solution.

Cytoplasmic Signals Are Required to Segregate VSVG Protein from Regulated Secretory Proteins

Experiments with VSV-infected GH3 pituitary cells showed that, in regulated secretory cells, constitutive release of VSVG protein from the TGN does not occur by default, but is strictly dependent on signal information in the cytoplasmic domain. The release of VSVG protein was inhibited by VSVG peptide with the same potency as in MDCK cells and 3T3 fibroblasts. In contrast, the release of GH and Prl was not affected by VSVGp. This latter result was surprising since in vivo experiments indicate that 70–80% of these two regulated secretory proteins are released constitutively in GH3 cells (Stoller and Shields, 1988). Two different scenarios may account for this observation. In the first scenario, the block of the major constitutive route by the VSVG peptide leads to more efficient packaging of the constitutively secreted fraction of GH and Prl into immature secretory granules (Fig. 9). In the second scenario, GH and Prl are transported via a secondary constitutive pathway to the cell surface that is insensitive to VSVGp, perhaps the equivalent of the apical pathway of epithelial cells. In fact, Orci et al. (1987*a*) have shown that HA is transported through a pathway distinct from the regulated secretory route in neuroendocrine cells.

In summary, the results presented in this report support

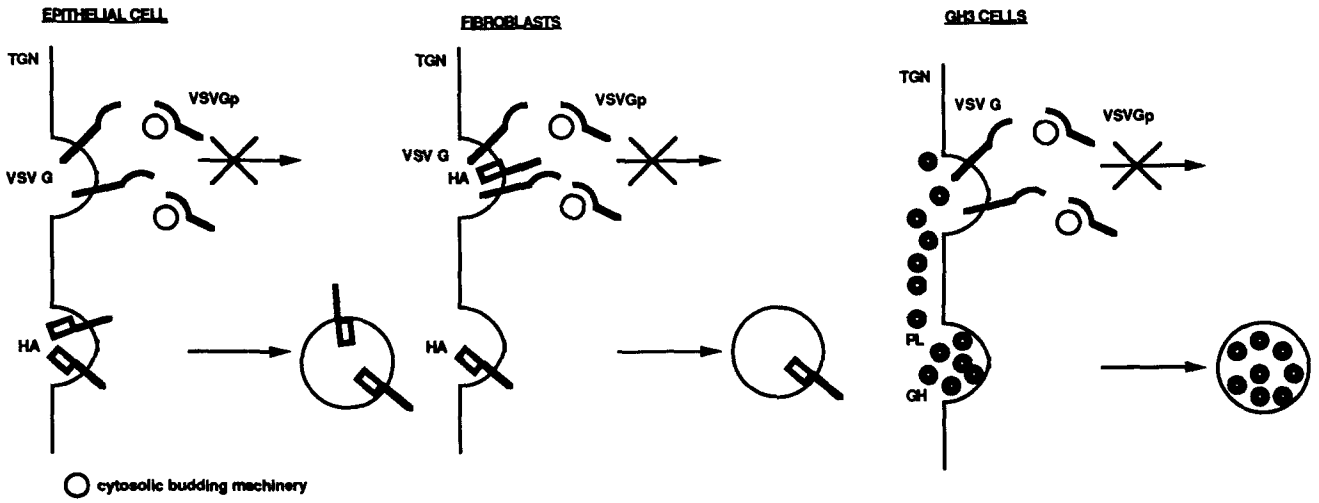

Figure 9. Models for the effect of VSVG peptide on the release of VSVG, HA, GH, and PL proteins in MDCK, 3T3, and GH3 cells. VSVG peptide competes in all three cell lines with the same soluble factor of the transport machinery that recognizes a signal in the cytoplasmic domain of VSVG protein resulting in the inhibition of the release of VSVG-containing vesicles. HA protein is excluded completely from VSVG-containing vesicles in MDCK cells and hence its transport is not affected. In nonpolarized 3T3 cells at least part of the HA molecules are transported via the same type of vesicles as the VSVG protein. In GH3 cells, Prolactin (*PL*) and growth hormone (*GH*) are chased efficiently into immature granules or into a different class of constitutive secreted vesicles than VSVG when the basolateral type of pathway is blocked.

a model in which VSVG protein is transported by the same signal-mediated mechanism in polarized and nonpolarized cells (Fig. 9). The requirement for signals excludes bulk flow as a mechanism for constitutive transport of proteins between the TGN and the cell surface in all cells. It also predicts the existence of cytosolic factors that interact with the basolateral-like signals in the cytoplasmic domain of the transported proteins. Our data also suggest the existence of an alternative apical-like pathway in 3T3 fibroblasts that is, however, considerably less developed than in MDCK cells and the existence of a basolateral signal independent pathway to the plasma membrane of GH3 cells. Thus, the existence of more than one pathway to the cell surface appears to be a widely distributed property of mammalian cells.

We thank Arkady Elgort for expert technical help with the GH3 cell experiments, Leona Cohen-Gould for the excellent electron microscopic work, T. Söllner and J. Rothman for providing us initially with bovine brain cytosol, S. Pimplikar for the VSVGA19 peptide, K. Mostov for the antibody against Gαs, Kelley Moremen for the mannosidase II antiserum, Alfonso Gonzalez, Duncan Wilson, Pat Brennwald, and the ERB laboratory for helpful discussions.

This work was supported by National Institutes of Health grant GM34107-12 to E. Rodriguez-Boulan and DK21860 to D. Shields. This study was made possible (in part) by funds granted to A. Müsch through a fellowship program sponsored by the Charles H. Revson Foundation and a fellowship by the Deutscher Akademischer Austauschdienst.

Received for publication 26 September 1995 and in revised form 23 February 1996.

References

Austin, C.D., and D. Shields. 1996. Prosomatostatin processing in permeabilized cells. *J. Biol. Cell.* 271:1194–1199.

Alberts, B., D. Bray, J. Lewis, M. Raff, K. Roberts, and J.D. Watson. 1994. The Molecular Biology of the Cell. Garland Publishing, Inc. New York & London.

Apodaca, G., B. Aroeti, K. Tang, and K.E. Mostov. 1993. Brefeldin-A inhibits the delivery of the polymeric immunoglobulin receptor to the basolateral surface of MDCK cells. *J. Biol. Chem.* 268:20380–20385.

Aroeti, B., and K.E. Mostov. 1994. Polarized sorting of the polymeric immunoglobulin receptor in the exocytic and endocytic pathway is controlled by the same amino acids. *EMBO (Eur. Mol. Biol. Organ.) J.* 13:2297.

Aroeti, B., P.A. Kosen, I.D. Kuntz, F.E. Cohen, and K.E. Mostov. 1993. Mutational and secondary structure analysis of the basolateral sorting signal of the polymeric immunoglobulin receptor. *J. Cell Biol.* 123:1149–1160.

Arvan, P., and D. Castle. 1992. Protein sorting and secretion granules formation in regulated secretory cells. *Trends Cell Biol.* 2:327–331.

Bauernfeind, R., and W. Huttner. 1993. Biogenesis of constitutive secretory vesicles, secretory granules and synaptic vesicles. *Curr. Opin. Cell Biol.* 5: 628–635.

Beckers, C.J.M., D.S. Keller, and W.E. Balch. 1987. Semi-intact cells permeable to macromolecules: use in reconstitution of protein transport from the endoplasmic reticulum to the golgi complex. *Cell.* 50:523–534.

Bomsel, M., and K.E. Mostov. 1993. Possible role of both the a and bg subunits of the heterotrimeric G protein, Gs, in transcytosis of the polymeric immunoglobulin receptor. *J. Biol. Chem.* 268:25824–25835.

Brewer, C.B., and M.G. Roth. 1991. A single amino acid change in the cytoplasmic domain alters the polarized delivery of influenza viral hemagglutin. *J. Cell Biol.* 114:413–421.

Casanova, J.E., G. Apodaca, and K.E. Mostov. 1991. An autonomous signal for basolateral sorting in the cytoplasmic domain of the polymeric immunoglobulin receptor. *Cell.* 66:65–75.

Chanat, E., and W. Huttner. 1992. Milieu-induced, selective aggregation of regulated secretory proteins in the *trans*-Golgi network. *J. Cell. Biol.* 115:1505–1519.

Chege, N.W., and S.R. Pfeffer. 1990. Compartmentation of the Golgi complex: brefeldin-A distinguishes *trans*-Golgi cisternae from the trans-Golgi network. *J. Cell. Biol.* 111:893–899.

Chung, K.N., P. Walter, G.W. Aponte, and H.P.H. Moore. 1987. Molecular sorting in the secretory pathway. *Science (Wash. DC).* 243:192–197.

Etchison, J.R., J.S. Robertson, and D.F. Summers. 1977. Partial structural analysis of the oligosaccharide moieties of the vesicular stomatitis virus glycoprotein by sequential chemical and enzymatic degradation. *Virology.* 78:375–392.

Gonzalez, A., L. Rizzolo, M. Rindler, M. Adesnik, D.D. Sabatini, and T. Gottlieb. 1987. Nonpolarized secretion of truncated forms of the influenza hemagglutinin and the vesicular stomatitis virus G protein from MDCK cells. *Proc. Natl. Acad. Sci. USA.* 84:3738–3742.

Green, R., and D. Shields. 1984. Somatostatin discriminates between the intracellular pathways of secretory and membrane proteins. *J. Cell Biol.* 99:97–104.

Griffiths, G., and K. Simons. 1986. The trans Golgi network: sorting at the exit site of the Golgi complex. *Science (Wash. DC).* 234:438–443.

Griffiths, G., B. Hoflack, K. Simons, I. Mellman, and S. Kornfeld. 1988. The mannose 6-phosphate receptor and the biogenesis of lysosomes. *Cell.* 52: 329–341.

Humphrey, J.S., P.J. Peters, L.C. Yuan, and J.S. Bonifacino. 1993. Localization of TGN38 to the *trans*-Golgi network: involvement of a cytoplasmic tyrosine-containing sequence. *J. Cell Biol.* 120:1123–1135.

Hunziker, W., C. Harter, K. Matter, and I. Mellman. 1991. Basolateral sorting in MDCK cells requires a distinct cytoplasmic domain determinant. *Cell.* 66: 907–920.

Kornfeld, R., and S. Kornfeld. 1985. Assembly of asparagine linked oligosaccharides. *Annu. Rev. Biochem.* 54:631–664.

Kreis, T.E. 1986. Microinjected antibodies against the cytoplasmic domain of vesicular stomatitis virus glycoprotein block its transport to the cell surface. *EMBO (Eur. Mol. Biol. Organ.) J.* 5:931–941.

Kuliawat, R., and P. Arvan. 1994. Distinct molecular mechanisms for protein sorting within immature granules of pancreatic β-cells. *J. Cell Biol.* 126:77–86.

Laemmli, U.K. 1970. Cleavage of structural proteins during assembly of the head of bacteriophage T4. *Nature (Lond.).* 227:680–685.

Le Bivic, A., Y. Sambuy, A. Patzak, N. Patil, M. Chao, and E. Rodriguez-Boulan. 1991. An internal deletion in the cytoplasmic tail reverses the apical localization of human NGF receptor in transfected MDCK cells. *J. Cell Biol.* 115:607–618.

Lisanti, M.P., and E. Rodriguez-Boulan. 1990. Glycophospholipid membrane anchoring provides clues to the mechanism of protein sorting in polarized epithelial cells. *TBIS (Trends. Biochem. Sci.)* 15:113–118.

Ludwig, T., R. LeBorgne, and B. Hoflak. 1995. Roles for mannose-6-phosphate receptors in lysosomal enzyme sorting, IGF-II binding and clathrin-coat assembly. *Trends Cell Biol.* 5:202–206.

Malhotra, V., T. Serafini, L. Orci, J.C. Shephard, and J.E. Rothman. 1989. Purification of a novel class of coated vesicles mediating biosynthetic protein transport throuh the Golgi stack. *Cell.* 58:329–336.

Matlin, K.S., and K. Simons. 1984. Sorting of an apical plasma membrane glycoprotein occurs before it reaches the cell surface in cultured epithelial cells. *J. Cell Biol.* 99:2131–2139.

Matter, K., and I. Mellman. 1994. Mechanisms of cell polarity: sorting and transport in epithelial cells. *Curr. Opin. Cell Biol.* 6:545–554.

Matter, K., W. Hunziker, and I. Mellman. 1992. Basolateral sorting of LDL receptor in MDCK cells: the cytoplasmic domain contains two tyrosine-dependent targeting determinants. *Cell.* 71:741–753.

Melancon, P., A. Franzusoff, and K.E. Howell. 1991. Vesicle budding: insight from cell free assays. *Trends Cell Biol.* 1:165–171.

Moore, H.-P.H., and R.B. Kelly. 1985. Secretory protein targeting in a pituitary cell line: differential transport of foreign secretory proteins to distinct secretory pathways. *J. Cell Biol.* 101:1773–1781.

Moremen, K.W., O. Touster, and P.W. Robbins. 1991. Novel purification of the catalytic domain of Golgi α-mannosidase II: characterization and comparison with the intact enzyme. *J. Biol. Chem.* 266:16876–16885.

Mostov, K.E., P. Breitfeld, and J.M. Harris. 1987. An anchor-minus form of the polymeric immunoglobulin receptor is secreted predominantly apically in Madin-Darby canine kidney cells. *J. Cell Biol.* 105:2031–2036.

Nabi, I.R., A. Le Bivic, D. Fambrough, and E. Rodriguez-Boulan. 1991. An endogenous MDCK lysosomal membrane glycoprotein is targeted basolaterally before delivery to lysosomes. *J. Cell Biol.* 115:1573–1584.

Orci, L., B.S Glick, and J.E. Rothman. 1986. A new type of coated vesicular carrier that appears not to contain clathrin: its possible role in protein transport within the Golgi stack. *Cell.* 46:171–184.

Orci, L., M. Ravazzola, M. Amherdt, A. Perrelet, S.K. Powell, D.L. Quinn, and H.-P. Moore. 1987*a*. The trans-most cisternae of the Golgi complex: a compartment for sorting of secretory and plasma membrane proteins. *Cell.* 51: 1039–1051.

Orci, L., M. Ravazzola, M.J. Storch, R.J. Anderson, J.D. Vassalli, and A. Perrelet. 1987*b*. Proteolytic maturation of insulin is a post-Golgi event which occurs in acidifying clathrin-coated secretory vesicles. *Cell* 49:865–868.

Pimplikar, S.W., and K. Simons. 1993. Regulation of apical transport in epithelial cells by a Gs class of heterotrimeric G protein. *Nature (Lond.).* 362:456–458.

Pimplikar, S.W., E. Ikonen, and K. Simons. 1994. Basolateral protein transport in streptolysin O–permeabilized MDCK cells. *J. Cell Biol.* 125:1025–1035.

Rajasekaran, A.K., J.S. Humphrey, M. Wagner, G. Miesenbock, A. Le Bivic, J.S. Bonifacino, and E. Rodriguez-Boulan. 1994. TGN38 recycles basolaterally in polarized Madin-Darby canine kidney cells. *Mol. Biol. Cell.* 5:1093–1103.

Rindler, M.J., I.E. Ivanov, H. Plesken, E. Rodriguez-Boulan, and D.D. Sabatini. 1984. Viral glycoproteins destined for apical or basolateral plasma membrane domains traverse the same Golgi apparatus during their intracellular transport in doubly infected Madin-Darby canine kidney cells. *J. Cell Biol.* 98:1304–1319.

Rodriguez-Boulan, E., and S.K. Powell. 1992. Polarity of epithelial and neuronal cells. *Annu. Rev. Cell Biol.* 8:395–427.

Rodriguez-Boulan, E., and D.D. Sabatini. 1978. Asymmetric budding of viruses in epithelial monolayers: a model system for study of epithelial polarity. *Proc. Natl. Acad. Sci. USA.* 75:5071–5075.

Rose, J.K., and J.E. Bergmann. 1983. Altered cytoplasmic domains affect intracellular transport of the vesicular stomatitis virus glycoprotein. *Cell.* 34:513–524.

Roth, J., D.J. Taatjes, J.M. Lucocq, J. Weinstein, and J.C. Paulson. 1985. Demonstration of an extensive trans-tubular network continuous with the Golgi apparatus stack that may function in glycosylation. *Cell.* 43:287–295.

Roth, M.G., C. Doyle, J. Sambrook, and M.J. Gething. 1986. Heterologous transmembrane and cytoplasmic domains direct functional chimeric influenza virus hemagglutinins into the endocytic pathway. *J. Cell Biol.* 102:1271–1283.

Rubin, L.A., C.C. Kurman, W.E. Biddison, N.D. Goldman, and D.L. Nelson. 1985. A monoclonal antibody 7G7/B6 binds to an epitope on the human interleuIC50n-2 (IL-2) receptor that is distinct from that recognized by IL-2 or anti-Tac. *Hybridoma.* 4:91–104.

Simons, K., and A. Wandinger-Ness. 1990. Polarized sorting in epithelia. *Cell.* 62:207–210.

Stoller, T.J., and D. Shields. 1988. Retrovirus-mediated expression of preprosomatostatin: posttranslational processing, intracellular storage, and secretion in GH3 pituitary cells. *J. Cell Biol.* 107:2087–2095.

Stoller, T.J., and D. Shields. 1989. The propeptide of presomatostatin mediates intracellular transport and secretion of α-globin from mammalian cells. *J. Cell Biol.* 108:1647–1655.

Tarantino, A.L., R.B. Trimble, and F. Maley. 1978. Endo-beta-.N-acetylglucosaminidase from *Streptomyces plicatus. Methods Enzymol.* 50:574–580.

Thomas, D.C., and M.G. Roth. 1994. The basolateral targeting signal in the cytoplasmic domain of glycoprotein G from vesicular stomatitis virus resembles a variety if intracellular targeting motifs related by primary sequence but having diverse targeting activities. *J. Biol. Chem.* 269:15732–15739.

Thomas, D.C., C.B. Brewer, and M.G. Roth. 1993. Vesicular stomatitis virus glycoprotein contains a dominant cytoplasmic basolateral sorting signal dependent upon a tyrosine. *J. Biol. Chem.* 268:3313–3320.

Tooze, J., and S.A. Tooze. 1986. Clathrin-coated vesicular transport of secretory proteins during the formation of ACTH-containing secretory granules in AtT20 cells. *J. Cell Biol.* 103:839–850.

Tooze, S.A., and W.B. Huttner. 1990. Cell-free protein sorting to the regulated and constitutive secretory pathways. *Cell.* 60:837–847.

van Meer, G., and K. Simons. 1988. Lipid polarity and sorting in epithelial cells. *J. Cell Biochem.* 36:51–58.

Wandinger-Ness, A., M.K. Bennett, C. Antony, and K. Simons. 1990. Distinct transport vesicles mediate the delivery of plasma membrane proteins to the apical and basolateral domains of MDCK cells. *J. Cell Biol.* 111:987–1000.

Wieland, F.T., M.L. Gleason, T.A. Serafini, and J.E. Rothman. 1987. The rate of bulk flow from the endoplasmic reticulum to the cell surface. *Cell.* 50:289–300.

Xu, H., and D. Shields. 1993. Prohormone processing in the *trans*-Golgi network: endoproteolytic cleavage of prosomatostatin and formation of nascent secretory vesicles in permeabilized cells. *J. Cell Biol.* 6:1169–1184.